Evolved Gas Analysis Investigation of the Reaction between Tris(2,4-pentanedionato)aluminum and Water Vapor in Chemical Vapor Deposition Processes To Produce Alumina

M. C. Rhoten and T. C. DeVore*

Department of Chemistry, James Madison University, Harrisonburg, Virginia 22807

Received September 27, 1996. Revised Manuscript Received May 20, 1997[⊗]

Evolved gas analysis−Fourier transform infrared spectroscopy was used to investigate the pyrolysis of tris(2,4-pentanedionato)aluminum on glass surfaces between 500 and 900 K in vacuum and in low-pressure water vapor atmospheres. Pyrolysis of tris(2,4-pentanedionato)aluminum in vacuum produced Al_2O_3, carbon, water vapor, and several volatile organic products. This pyrolysis is surface enhanced and has an apparent activation energy of ∼100 kJ/mol. Water vapor reacted with the tris(2,4-pentanedionato)aluminum to form 2,4-pentanedione and Al_2O_3. Largely pure Al_2O_3 was formed between 600 and 700 K in a water vapor atmosphere. This reaction was first order in the water vapor pressure. The order in tris(2,4-pentanedionato)aluminum was modeled well by the Langmuir adsorption isotherm. The apparent activation energy for the production of 2,4-pentanedione varied with the reaction conditions and had a lower limit of ∼28 kJ/mol when the reaction was run in excess water vapor. Possible reaction sequences are given for each case. The formation of $Al(C_5H_7O_2)_2OH$ is postulated to be a reaction intermediate during each sequence. This intermediate has not been isolated.

Introduction

Amorphous aluminum oxide films are widely used for a variety of practical applications such as gate insulators and protective layers on silicon in semiconductors.[1] Since tris(2,4-pentanedionato)aluminum [$Al(C_5H_7O_2)_3$] is nontoxic and easily handled in solid form at room temperature, it has been used to prepare amorphous aluminum oxide thin films on glass substrates via chemical vapor deposition processes.[1−10] Ajaya et al.[7] used atmospheric pressure pyrolysis of $Al(C_5H_7O_2)_3$ in argon atmospheres to deposit amorphous aluminum oxide films on glass substrates heated above 690 K. Korzo et al.[8] prepared amorphous aluminum oxide films on silicon substrates using the vacuum pyrolysis of $Al(C_5H_7O_2)_3$ at temperatures above 725 K. In each case the films contained a slight excess of oxygen and were contaminated with carbon. Maruyama and Arai[9] found that pyrolysis of $Al(C_5H_7O_2)_3$ in air produced largely carbon-free aluminum oxide films with substrate temperatures as low as 625 K. They reported an activation energy of 28 kJ mol^{-1} for this process. Kim et al.[10] concluded that adding water vapor to the reaction mixture produced carbon-free aluminum oxide films on soda lime glass or on silicon (100) with substrate temperatures as low as 600 K. Since the water vapor significantly increased the film growth rate, they hypothesized that the water contributed to the transport of the organic material away from the reaction surface or else that it reacted with the $Al(C_5H_7O_2)_3$ to form a volatile metastable product that decomposed on the substrate. Further details for this mechanism were not established.

Solid $Al(C_5H_7O_2)_3$ sublimes without decomposition in reduced pressure environments. Three investigations (including the preliminary report of this research)[11] of the thermal decomposition of $Al(C_5H_7O_2)_3$ vapor have been published.[11−13] Minkina[12] investigated this decomposition under static conditions at temperatures between 653 and 723 K and $Al(C_5H_7O_2)_3$ pressures between 6.5 and 13.3 kPa. The reaction rate was largely independent of the initial pressure of $Al(C_5H_7O_2)_3$. Since there was an induction period for the reaction at the lower temperatures and packing the reaction vessel with solid pyrolysis products or crushed glass tubing increased the rate of reaction. Minkina concluded that the reaction was surface catalyzed and that the products were better catalysts than glass. The activation energy was determined to be 103 ± 4 kJ/mol. Mass spectrometric analysis of the gaseous mixture formed during

[⊗] Abstract published in *Advance ACS Abstracts,* July 1, 1997.

(1) Pierson, H. O. *Handbook of Chemical Vapor Deposition: Principles, Technology and Applications*; Noyes Publications: Park Ridge, NJ, 1992.
(2) Korzo, V. F. *Zh. Prikl. Khim. (Leningrad)* **1976**, *49*, 74−7.
(3) Sokolowski, M.; Sokolowska, A.; Michalski, A.; Ziolkowski, Z *J. Cryst. Growth* **1981**, *52*, 274−8.
(4) Rabinovich, V. G. *Izv. Akad. Nauk SSSR, Neorg. Mater.* **1981**, *17*, 1008−11.
(5) Poston, S.; Reisman. A. *J. Electron. Mater.* **1989**, *18*, 79−84.
(6) Mittov, O. N.; Fetisova, S. V.; Gadebshaga, T. A.; Nevryuev, I. I.; Agapov, B. L. *Izv. Akad. Nauk SSSR, Neorg. Mater.* **1991**, *27*, 893−6.
(7) Ajayi, O. B.; Akanni, M. S.; Lambi, J. N.; Burrows, H. D.; Osasena, O.; Podor, B. *Thin Solid Films* **1986**, *138*, 91−95.
(8) Korzo, V. F.; Ibraimov, N. S.; Galkin, B. D. *J. Appl. Phys.* **1969**, *42*, 989.
(9) Maruyama, T.; Arai, S. *Appl. Phys. Lett.* **1992**, *60*, 322−323.
(10) Kim, J. S.; Marzouk, H. A.; Reucroft, P. J.; Robertson, J. D.; Hamrin, Jr., C. E. *Appl. Phys. Lett.* **1993**, *62*, 681−683.
(11) Crouch, M. A.; DeVore, T. C. *Proceedings of the Eighth National Conference on Undergraduate Research*; Yearout, R. D., Ed.; The University of North Carolina: Ashville, NC, 1994; Vol. III, p 1029.
(12) Minkina, V. G. *Inorg. Mater.* **1993**, *29*, 1400−1401.
(13) Bykov, A. F.; Turgambaeva, A. E.; Igumenov, I. K.; Semyannikov, P. P. *J. Phys. IV* **1995**, *C5*, C5/191−C5/197.

S0897-4756(96)00504-2 CCC: $14.00

the reaction indicated that 12 gaseous products were produced. 2-Propanone (44.67%) and carbon dioxide (33.81%) were the most abundant. The orange-claret film that coated the reactor walls at the conclusion of the experiment was not analyzed. Bykov et al.[13] used a mass spectrometer to monitor the products leaving a flow reactor. 2,4-Pentanedione, 2-propanone, ketene (C_2H_2O), and unidentified compounds with formulas of C_5H_6O, $C_{10}H_{12}O_2$, and $C_8H_{10}O$ were observed in the mass spectrum. They proposed that the decomposition followed three parallel routes and presented reaction schemes for each. The reaction was analyzed by assuming that it followed first-order kinetics and had an activation energy of 83.8 kJ/mol.

Evolved gas analysis−Fourier transform infrared spectroscopy has been used to investigate the thermal decomposition of $Al(C_5H_7O_2)_3$ vapor in vacuo and in low-pressure water vapor atmospheres at temperatures between 500 and 900 K. These experiments have established that the enhanced growth rate reported by Kim et al.[10] resulted from the reaction between $Al(C_5H_7O_2)_3$ and water vapor to produce Al_2O_3 and 2,4-pentanedione:

$$2Al(C_5H_7O_2)_3 + 3H_2O \rightarrow Al_2O_3 + 6C_5H_8O_2 \quad (1)$$

$Al(C_5H_7O_2)_3$ thermally decomposes at temperatures above 570 K. This decomposition produced several volatile organic compounds and a dark nonvolatile residue. Heating the residue in air produced Al_2O_3. This behavior was consistent with the previous reports that the Al_2O_3 films produced from pyrolysis of $Al(C_5H_7O_2)_3$ are contaminated with carbon and that forming the film in air produced largely carbon-free Al_2O_3.[7−9]

Experimental Section

The experimental apparatus used is shown schematically in Figure 1. The IR cell, which has been described in detail previously,[11,14−16] was constructed from a stainless steel four-way cross vacuum flange (MDC Corp.). One leg of this flange was connected to the vacuum system using a bellows valve. The approximately 10 cm long optical path was formed by attaching KBr windows to the two remaining opposing legs of the flange with O-ring connectors. The reactor was connected to the IR cell through the remaining connection port using a Cajon 316 tube connector that has been silver soldered into a blank vacuum flange. A furnace assembly, constructed by wrapping a Vycor tube with nichrome heating wire and thermal insulation, slipped over the reactor and was used to heat the sample. The temperature of the cell was monitored with a chromel−alumel thermocouple connected to a Keithley digital thermometer. For 0.1−0.2 g samples, the temperature of the sample can be determined to ±3 K. Averages of several experiments were used to attempt to minimize the effects of the uncertainty of the temperature measurements on the final results.

All experiments were done using the two-furnace arrangement shown in Figure 1. The reactor was constructed from a 30−40 cm long piece of glass tubing. One end was attached to the IR cell, and the other was attached to a glass vial containing liquid water. A Teflon needle valve was used to control the flow of water vapor into the system. The $Al(C_5H_7O_2)_3$ was placed approximately 10 cm from the end of the tube connected to the water vial. It occupied a region of the tube approximately 0.5−1 cm long and was held in place using glass wool. The $Al(C_5H_7O_2)_3$ was sublimed using the first furnace, and the vapor was mixed with water vapor. This mixture flowed down the sample tube at the vaporization temperature for approximately 2 cm before entering the reaction zone. The 5−7 cm long reaction zone was heated with the second furnace. The nonvolatile products condensed on the sample tube in this region while the volatile products were pulled along the rest of the tube (~20 cm) by using a dynamic vacuum. Since this part of the reactor was not heated, the less volatile products condensed on this part of the tube which kept the IR windows largely free of deposits during the reaction. The yellow residue that collected in the tube was dissolved in $CHCl_3$ and identified using gas chromatography−mass spectroscopy (GC-MS). Added water vapor flow rates between 0 and 1 dm^3/min (1 L/min) were used during these experiments. The intensity of the infrared water bands was used to monitor the amount of water flowing through the cell. No carrier gas was used during any of the experiments.

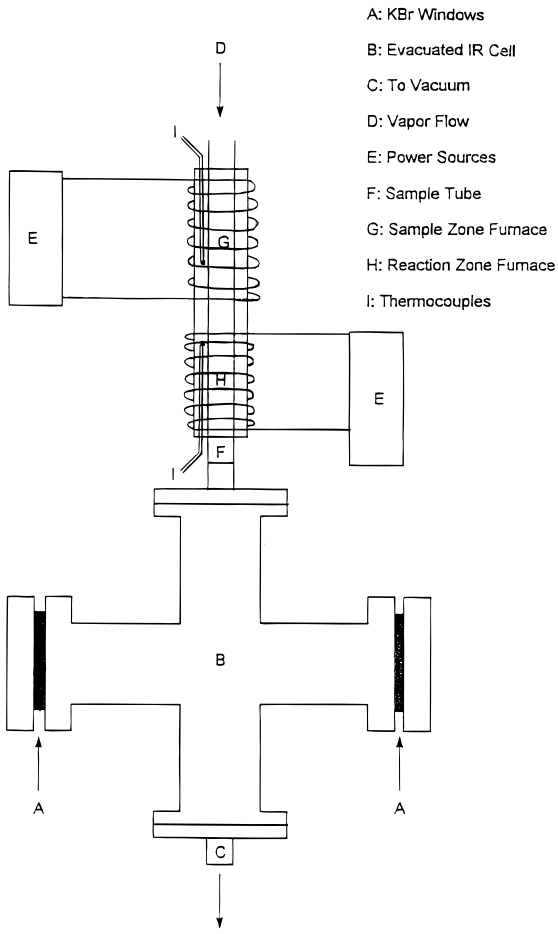

Figure 1. Schematic diagram of the stainless steel infrared cell used to investigate the reaction between tris(2,4-pentanedionato)aluminum and water vapor.

Since the temperature of each furnace was controlled independently, two experimental procedures were possible. In one, the temperature of the first furnace was held constant using a potentiostat. The temperature in the reaction zone was increased at a constant rate (4−8 K/min) by using a Perkin regulated power supply to control the heating rate. This provided a constant partial pressure of the complex and a nearly constant flow rate of the reactants through the reaction zone. The change in the extent of reaction as a function of temperature was obtained and used to determine the activation energy for the reaction. In the second procedure, the reaction temperature was fixed while the temperature used to sublime the metal complex was changed. This procedure monitored the changes in the reaction dynamics as a function of the complex partial pressure and provided information about the order of the reaction.

(14) Crouch, M. A.; DeVore, T. C. *Chem. Mater.* **1996**, *8*, 32−36.
(15) DeVore, T. C.; Gallaher, T. N. *High Temp. Sci.* **1983**, *16*, 269−275.
(16) DeVore, T. C.; Gallaher, T. N. *Inorg. Chem.* **1984**, *23*, 3506−3509.

Both types of experiment were done in a constant-flow reactor using a dynamic flow under a total pressure of approximately 6 Pa. It was assumed that the reaction occurred only while the reactants were in the hot zone of the reactor and that all species flowed through the reactor at a constant (but not necessarily the same) rate throughout the experiment. The rate of reaction was determined by using the differential method. In this method, the rate of reaction for a simple system

$$aA \rightarrow pP \tag{2}$$

is given by[17]

$$\text{rate} = -1/a(dA/dt) = 1/p(dP/dt) \tag{3}$$

In practice, neither absolute flow rates nor absolute rate constants were determined. The data were collected for several temperatures during a single experiment where constant-flow conditions had been established and experiments using several different sets of conditions were used to make the conclusions reported. Since only the reactants entered the reaction region, all of the products observed were assumed to have formed during the reaction. In this case, dP/dt is proportional to the absorbance of the characteristic infrared bands of the product molecules if the assumption that the compound flowed through the cell at a constant rate is valid. The flow rate is largely determined by the pressure gradient in the cell and the pumping speed. The pumping speed could be changed by attaching varying lengths of $^1/_4$ in. polyethene tubing between the cell and the vacuum system. The pressure at the vacuum end of the tube was monitored to determine if obvious changes in the flow of gas through the IR cell were occurring. No obvious differences were obtained when using lengths of tubing that varied by a factor of 3, suggesting that the assumption that the flow rate remained constant during the experiment was acceptable. The absorbance of the water vapor provided a convenient measurement of the water vapor pressure and the temperature used to sublime the $Al(C_5H_7O_2)_3$ was used to calculate the pressure of this compound entering the reactor.

The Nicolet 740 FTIR, used for these investigations, can collect and store one spectrum approximately every 2 s for reaction times up to 40 min. Each spectrum was collected from 400 to 4000 cm^{-1} with 4 cm^{-1} resolution. The Nicolet-Aldrich spectral library was used to help identify the composition of the evolved gases.

The GC-MS results were obtained using a Hewlett-Packard 5889 GC coupled to a HP 5971 series mass-sensitive detector. The column was an SPB-5. The sample was eluted using a variable temperature program that started at 313 K and increased to a final temperature 475 K at a rate of 10 K/min. The NBS mass spectral library was used to help identify the compounds.

Results and Discussion

The gas chromatogram of the volatile products collected in a liquid nitrogen trap while pyrolyzing $Al(C_5H_7O_2)_3$ at 825 K is shown in Figure 2. Peaks corresponding to seven different compounds have been identified. The more intense mass spectral peaks of each compound are given in Table 1. 2,4-Pentanedione was the most abundant species formed under these conditions. Three compounds, all with molecular formula C_5H_6O, and 2-propanone were the next most abundant species found. The GC-MS of the yellow residue that collected in the reactor is shown in Figure 3. The unique species that have been established are also given in Table 1. The largest peak is unreacted $Al(C_5H_7O_2)_3$. At least one isomer of dimethyl phenol,

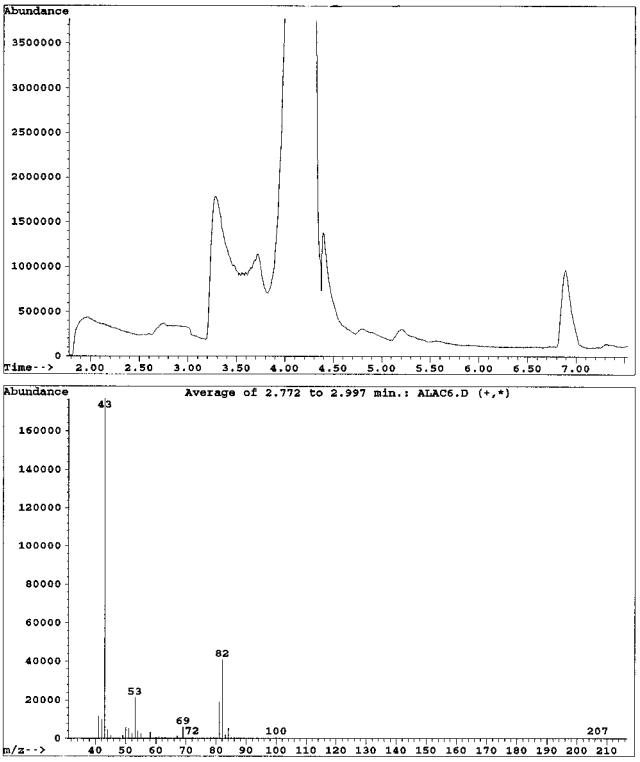

Figure 2. Gas chromatogram of the volatile products formed during the thermal decomposition of tris(2,4-pentanedionato)-aluminum. The products were collected in a glass trap cooled in liquid nitrogen. The main product (2,4-pentanedione) is shown off-scale to expand the size of the minor product peaks. A typical mass spectrum for a minor product is also shown in the figure.

Table 1. Chemical Compounds Identified in the GC-MS of the Products Formed from the Thermal Decomposition of Tris(2,4-pentanedionato)aluminum

retention time	significant mass peaks	possible assignment
2.0	58, 43	C_3H_6O (2-propanone)
2.8	82, 69, 53, 43	C_5H_6O (see text)
3.3	82, 67, 51, 43	C_5H_6O (see text)
3.7	82, 67, 51, 43	C_5H_6O (see text)
4.1	100, 85, 43	$C_5H_8O_2$ (2,4-pentanedione)
5.2	106, 91, 77	C_7H_6O (benzaldehyde)
6.9	120, 105, 77	C_8H_8O (aromatic?)
11.9	122, 107, 77	$C_8H_{10}O$ (dimethylphenol)
12.7	162, 119, 107, 77, 43	$C_{10}H_{10}O_2$ (aromatic?)
15.4	164, 149, 107	$C_{10}H_{10}O_2$ (C_5H_6O dimer)
15.7	164, 149, 107	$C_{10}H_{10}O_2$ (C_5H_6O dimer)
18.5	324, 225, 126, 27	$Al(C_5H_7O_2)_3$

an aromatic compound with formula $C_{10}H_{10}O_2$, and two isomers of $C_{10}H_{12}O_2$ were also identified. The mass spectra of these compounds also contained evidence that 2,4-pentanedione was being formed on the column. While it is not surprising that thermal decomposition or chemical reaction of the $Al(C_5H_7O_2)_3$ could occur on the column, this hindered the identification of the molecules in this solid, and many have produced some false product peaks.

IR spectra obtained for increasing reaction zone temperatures with a constant flow of $Al(C_5H_7O_2)_3$ vaporized at 410 K and no added water vapor are presented in Figure 4. 2,4-Pentanedione (characteristic IR frequency at 1625 cm^{-1}) was the only volatile product observed when the reaction zone temperature was 750 K, and the amount of this compound increased as the reaction temperature was raised. By 800 K, IR bands

(17) For example, see: Atkins, P. W. *Physical Chemistry*, 5th ed.; Freeman: New York, 1994.

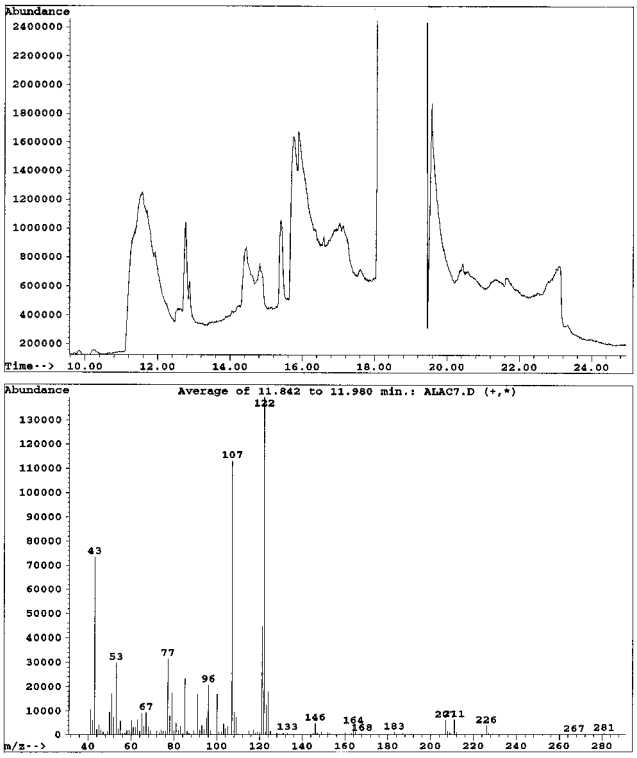

Figure 3. Gas chromatogram of the yellow residue that formed during the thermal decomposition of tris(2,4-pentanedionato)aluminum. The largest peak is from unreacted tris-(2,4-pentanedionato)aluminum. A typical mass spectrum for a minor product is also shown in the figure.

from a molecule with a characteristic IR frequencies at 1725 and 1945 cm^{-1} appeared. The band at 1725 cm^{-1} could be from the 2-propanone since this compound was observed in the mass spectrum. However, the frequency expected for 2-propanone is 1740 cm^{-1}. Since the 1725 cm^{-1} band correlates well with the 1945 cm^{-1} band, both frequencies could arise from the same molecule. The 1945 cm^{-1} band clearly resulted from a C≡C stretch or a C=C=C stretch and is most likely from the more abundant C_5H_6O molecule observed in the mass spectrum of the volatile products. The 1725 cm^{-1} could arise from the CH_3CO grouping indicated by the 43 dalton peak found in the mass spectrum of this compound (see Figure 2). Three possible isomers of C_5H_6O (1-pentyn-4-one, 3-pentyn-2-one, and 1,2-pentadien-4-one) are consistent with this IR spectrum and the mass spectrum. There is evidence for all three isomers in the GC-MS of the volatile products. Since 3-pentan-2-one can form from the thermal decomposition of a 2,4-pentanedionato ligand without a corresponding H atom migration, these IR frequencies are tentatively identified as arising from this isomer. CO_2 (characteristic IR frequency at 2340 cm^{-1}), ketene (C_2H_2O, characteristic IR frequency at 2150 cm^{-1}), and CH_4 (characteristic IR frequency at 3015 cm^{-1}) were identified when the temperature reached 825 K. When water vapor was added to the reaction mixture, 2,4-pentanedione was the dominant product formed at all temperatures. The intensity ratio for the 1625 cm^{-1} band relative to the 1725 cm^{-1} band at 850 K changed from 1.3 with minimal water to 4.9 when water vapor was added. These experiments suggested that water vapor promoted the production of 2,4-pentanedione relative to the other reaction products and that at least two reaction mechanisms were occurring.

IR spectra obtained using a constant reactor temperature of 835 K and varying pressures of the tris(2,4-pentanedionato)aluminum are shown in Figure 5. 3-Pentyne-2-one was observed at 375 K. Bands arising from ketene, 2,4-pentanedione, water vapor (characteristic IR pattern the 3500 cm^{-1} region), and methane were

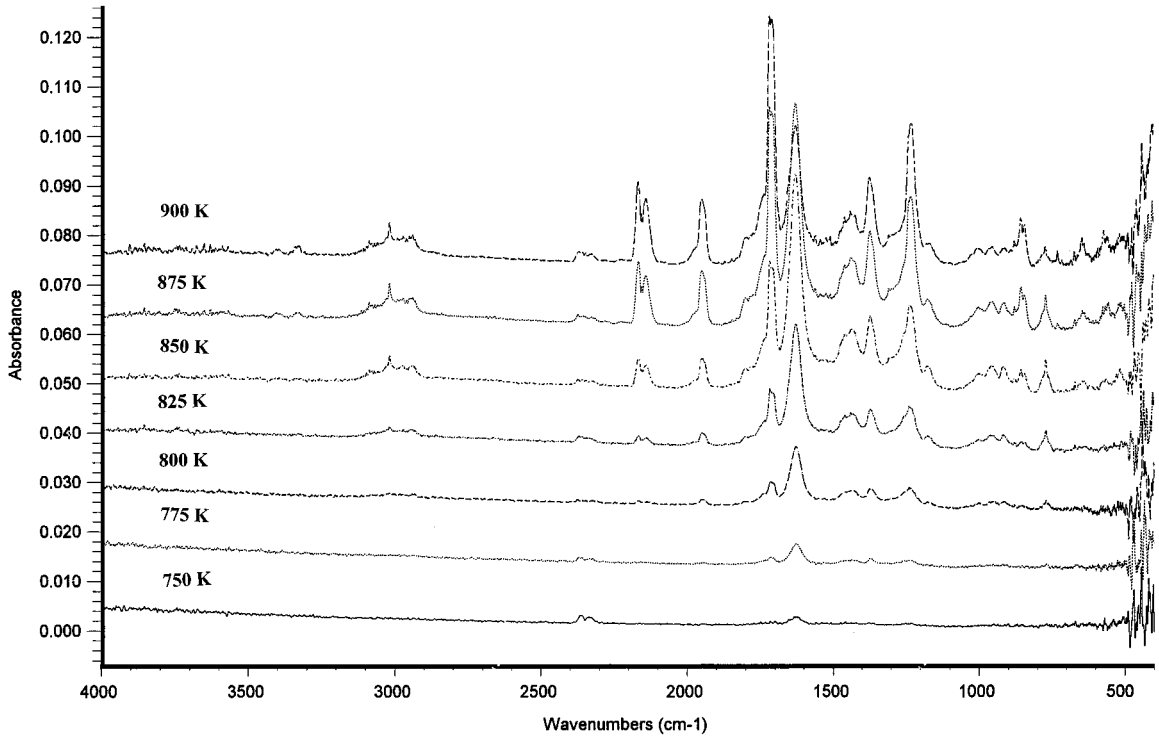

Figure 4. Collage of the IR spectra obtained from the reaction between tris(2,4-pentanedionato)aluminum and a trace of water vapor. The temperature in the reaction zone is given in the figure. The aluminum complex was vaporized at a constant temperature of 420 K.

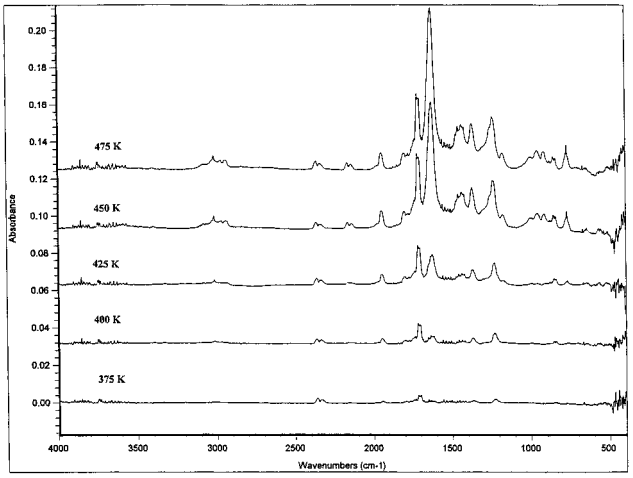

Figure 5. Collage of the IR spectra showing the effect of increasing the metal complex vapor pressure on the reaction between tris(2,4-pentanedionato)aluminum and water vapor. The aluminum complex vaporization temperatures are given in the figure. The reaction temperature was 850 K.

observed as the $Al(C_5H_7O_2)_3$ vaporization temperature was increased. The intensity of the characteristic infrared frequencies of all compounds increased as the partial pressure of the $Al(C_5H_7O_2)_3$ was raised, showing that the reaction depended upon the amount of $Al(C_5H_7O_2)_3$ in the system. The different rates of formation of each compound further indicated that at least two different reaction mechanisms were occurring.

Control experiments done by reacting water vapor and 2,4-pentanedione between 675 and 875 K produced no observable reaction. This confirmed that all of the observed reaction products were produced from reactions involving $Al(C_5H_7O_2)_3$.

These preliminary experiments suggested that water vapor reacted with $Al(C_5H_7O_2)_3$ to produce 2,4-pentanedione. The dependence of this reaction on the water vapor pressure was determined by keeping the vaporization temperature of the $Al(C_5H_7O_2)_3$ and the reaction zone temperature constant while adding different amounts of water vapor to the reactor. The results obtained are presented in Figure 6. The integrated intensity of the 2,4-pentanedione IR band increased linearly (or nearly so) as the integrated intensity of the IR band of water vapor increased; indicating that the reaction follows first-order kinetics with respect to the water vapor pressure.

The dependence of the reaction on the pressure of $Al(C_5H_7O_2)_3$ was determined by changing the vaporization temperature of $Al(C_5H_7O_2)_3$ while keeping the reaction zone temperature and the water vapor concentration constant. The amount of the 2,4-pentanedione produced did not follow a simple gas-phase kinetic model. While it was linearly dependent on the $Al(C_5H_7O_2)_3$ pressure at low $Al(C_5H_7O_2)_3$ vapor pressures, it was largely independent of the $Al(C_5H_7O_2)_3$ pressure at high $Al(C_5H_7O_2)_3$ vapor pressures. This observation indicates why Minkina[12] (zeroth order) and Bykov et al.[13] (first order) observed different reaction orders. This behavior is consistent with Langmuir surface-catalyzed kinetics[17] and supports Minkina's[12] conclusion that the reaction is occurring on the surface. In the simplest form of this mechanism, the reactant molecules adsorbed on the surface are in equilibrium with those in the gas phase. The adsorbed molecules decompose or

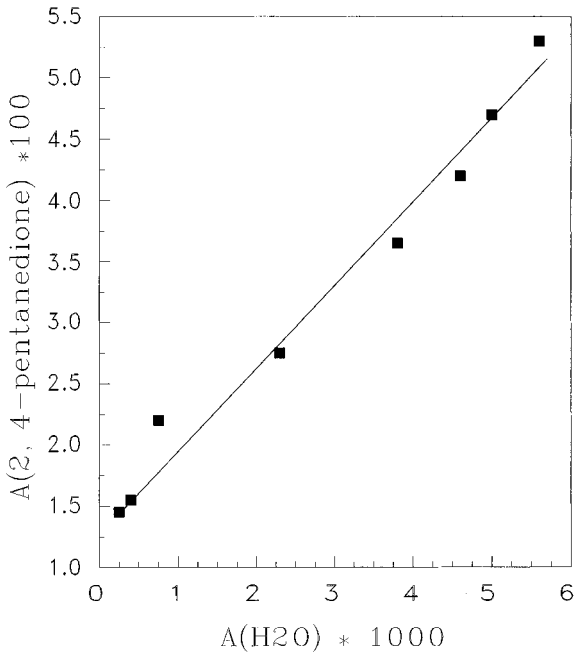

Figure 6. Comparison of the integrated intensity of the 1625 cm^{-1} IR band of the 2,4-pentanedione produced from the reaction between tris(2,4-pentanedionato)aluminum and water vapor and the integrated intensity of the 3500 cm^{-1} water vapor band. The reaction temperature was 645 K and the metal complex vapor pressure was 135 Pa.

react with other molecules in the system while on the surface. The products desorb and the process continues:

$$A(g) \leftrightarrow A(sur) \quad (4)$$

$$A(sur) (+B(g)) \rightarrow P(sur) \quad (5)$$

$$P(sur) \rightarrow P(g) \quad (6)$$

where A and B are reactants and P represents the products formed.

Assuming that step 5 is rate limiting, the reaction rate (ν) is proportional to the fraction of the surface occupied (θ) and the vapor pressure of compound B:

$$\nu = k_2 \theta P_B \quad (7)$$

where k_2 is the rate constant for step 5. The fraction of the surface occupied (θ) is given by the equilibrium process (4), and the rate expression (7) becomes[17]

$$\nu = k_2 P_B [K_1 P_A/(1 + K_1 P_A)] \quad (8)$$

This reaction follows first-order kinetics at relatively low pressures of A ($K_1 P_A \ll 1$) and zero-order kinetics at relatively high pressures of A ($K_1 P_A \gg 1$).

Further support that the reaction was occurring on the surface was obtained by packing the reaction zone with glass beads or glass helixes to increase the surface area. The amount of 2,4-pentanedione produced clearly increased and higher $Al(C_5H_7O_2)_3$ pressures were needed to reach the zeroth-order reaction region.

The most convenient form of the test for this mechanism is obtained by taking the reciprocal of eq 8 and multiplying both sides by P_A to give

$$P_A/\nu = 1/k_2 P_B K_1 + P_A/k_2 P_B K_1 \quad (9)$$

Since the reactants are flowing through a fixed length

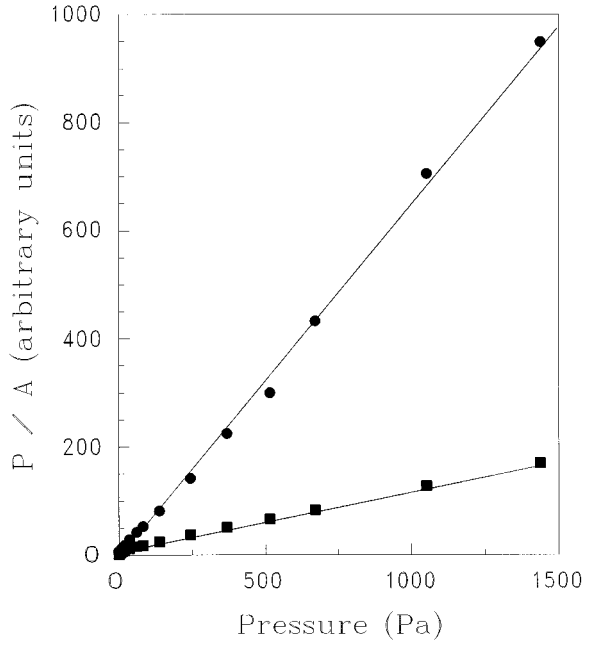

Figure 7. Plot of the pressure of the tris(2,4-pentanedionato)-aluminum divided by the absorbance of the product band versus the pressure of the tris(2,4-pentanedionato)aluminum. A linear relationship is consistent with the langmuir adsorption isotherm mechanism (see text). The squares were determined using the 1624 cm^{-1} band of 2,4-pentanedione, and the circles were made using the 1725 cm^{-1} band of C_5H_6O.

of reactor at a fixed flow rate during each experiment, the rate of reaction (v) is directly proportional to the IR absorbance of the product. Hence, a plot of P_A/absorbance of the product molecule versus P_A should give a straight line if this mechanism is followed. Rate plots[17] for the formation of 2,4-pentanedione and the 1725 cm^{-1} band made by assuming that the reaction followed the simple Langmuir adsorption mechanism are given in Figure 7. These plots were linear for all but the lowest $Al(C_5H_7O_2)_3$ vapor pressures. The marked negative deviation of the 2,4-pentanedione plot at low pressures is consistent with Minkina's observation[12] that the reaction is more efficiently catalyzed by the products (probably Al_2O_3) than by the glass. The rate of reaction would then be expected to increase rapidly until the surface is coated with the product and the steady-state conditions predicted by the Langmuir equation are reached.

It should be possible to determine the activation energy for each process by keeping the $Al(C_5H_7O_2)_3$ and the water vapor pressures constant and changing the reaction zone temperature. As shown in Figure 8, reasonable Arrhenius plots were obtained for any single set of experimental conditions and plots of the logarithm of the absorbance of each product versus the reciprocal of the temperature are linear in the low-temperature region. The near-zero slope at elevated temperatures is also expected and resulted from the total conversion of the $Al(C_5H_7O_2)_3$ to products. Once the reaction becomes quantitative, no further increase the amount of products formed can occur as the temperature is raised. However, the apparent activation energy changed markedly as the experimental conditions were changed (see Figure 9). The values obtained ranged from over 100 kJ/mol when no water was added to ~28 kJ/mol at the highest water vapor flows used. As shown in Figure

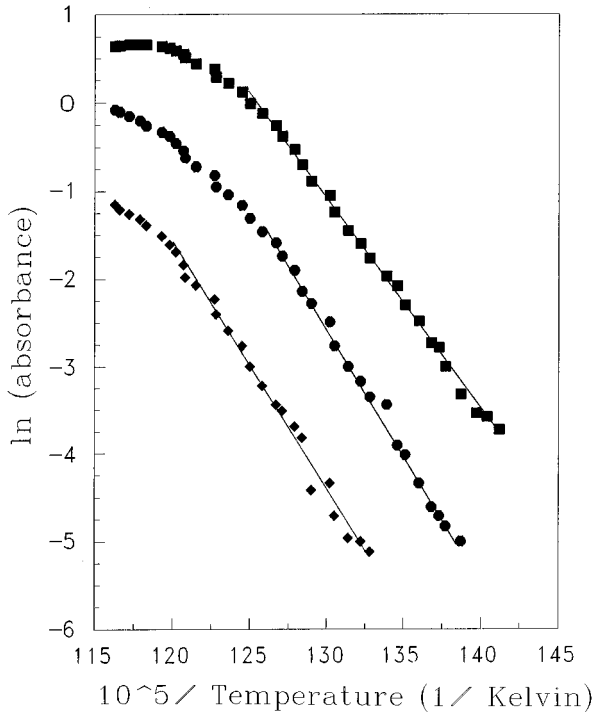

Figure 8. Arrhenius plots made for 2,4-pentanedione (squares), C_5H_6O (circles), and ketene (diamonds). The $Al(C_5H_7O_2)_3$ vaporization temperature was 410 K. No water was added in this experiment.

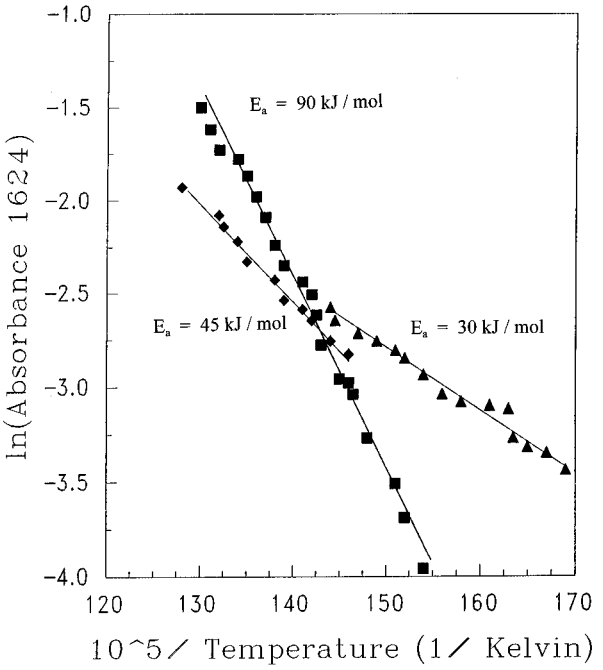

Figure 9. Typical Arrhenius plots obtained in the linear region for the formation of 2,4-pentanedione as the amount of water vapor added to the cell decreased. The apparent activation energies are given in the figure.

10, there was a relationship between the apparent activation energy observed and the amount of water vapor passing through the reaction region. Since precise measurements of the absorbance of the water vapor in the system could not be made, the absorbance of the 2,4-pentanedione produced at a fixed reaction temperature divided by the vapor pressure of the $Al(C_5H_7O_2)_3$ was used to estimate the water vapor pressure in the system in Figure 10. The reaction is first order in both

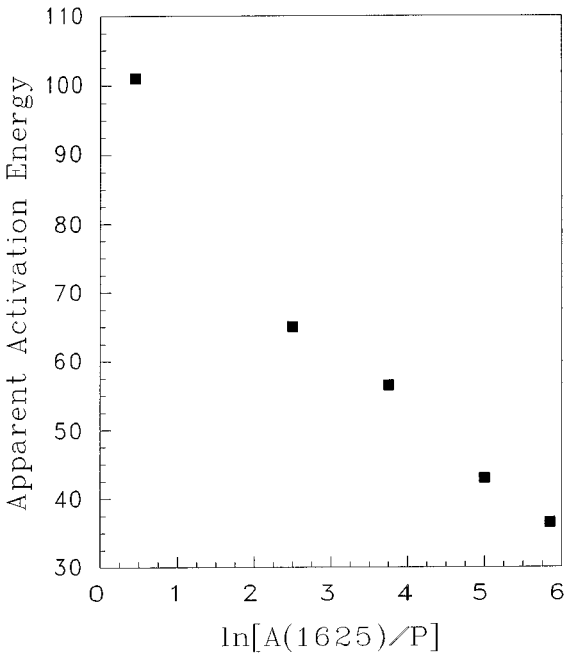

Figure 10. Changes in the apparent activation energy for the reaction between tris(2,4-pentanedionato)aluminum and water vapor as the extent of reaction changes. The natural logarithm of the absorbance of the 2,4-pentanedione divided by the vapor pressure of the tris(2,4-pentanedionato)aluminum is used to reflect the amount of water vapor in the system (see text).

the water vapor pressure and the $Al(C_5H_7O_2)_3$ vapor pressure at low $Al(C_5H_7O_2)_3$ pressures. Rearranging eq 8 in the low P_A limit and using the absorbance of 2,4-pentanedione to measure the rate of reaction shows that this function approximates the water vapor pressure:

$$P_B \sim A_{1624}/k_2K_1P_A \quad (10)$$

An increasing ratio of A_{1624}/P_A corresponds to an increasing amount of water vapor in the system. A nearly linear relationship was observed for a plot of the apparent activation energy and the logarithm of this function. While the exact meaning of this relationship has not been established, it clearly showed that the amount of water vapor in the system influenced the apparent activation energy in a predictable manner.

One possible explanation for the changing apparent activation energy for the production of the 2,4-pentanedione is that it formed from more than one pathway. For example, if the 2,4-pentanedione formed from a direct decomposition pathway and from a pathway involving the reaction with water:

$$Al(C_5H_7O_2)_3 \rightarrow C_5H_8O_2 + \text{other products} \quad (11)$$

$$dP[Al(C_5H_7O_2)_3]/dt = k_1P[Al(C_5H_7O_2)_3]$$

$$Al(C_5H_7O_2)_3 + H_2O \rightarrow C_5H_8O_2 + \text{other products} \quad (12)$$

$$d[Al(C_5H_7O_2)_3]/dt = k_2P[H_2O]P[Al(C_5H_7O_2)_3]$$

the observed rate of formation of 2,4-pentanedione would be given by the sum of these processes

$$dP[Al(C_5H_7O_2)_3]/dt = \{k_1 + k_2P[H_2O]\}P[Al(C_5H_7O_2)_3] \quad (13)$$

If the concentration of H_2O is low enough, $k_1 >> k_2P[H_2O]$, the activation energy determined would approach the activation energy for the direct pyrolysis step. Similarly, if $k_2P[H_2O] >> k_1$, the activation energy determined would approach the activation energy for the hydrolysis reaction. If $k_1 \sim k_2P[H_2O]$, both would contribute and the activation energy determined would be an intermediate value. (The Arrhenius plots should be linear only at the limits, and some curvature is expected when $k_1 \sim k_2P[H_2O]$. Computer simulations show that the deviation will be concave upward over long temperature ranges with the greatest nonlinearity in the region where the curves cross. However, the curves over short temperature ranges that do not include the crossing point are nearly linear with slopes that differ from either parent curve. As shown in Figures 8 and 9, the scatter in the data, the small effective temperature ranges caused by using low $Al(C_5H_7O_2)_3$ vapor pressures, and the concave downward deviations caused by surface effects made it difficult to establish the extent of the nonlinearity in the intermediate plots.) While the details of the mechanism need some refinement, this model is consistent with the observed data. The limiting value found in water vapor atmospheres (28 kJ/mol) agrees with the value reported by Maruyama and Arai[9] for the deposition of Al_2O_3 in air and is a reasonable estimate for the activation energy of the water reaction path. An activation energy of over 100 kJ/mol for the direct pyrolysis path agrees with the activation energy of 103 kJ/mol reported by Minkina.[12]

The direct decomposition of $Al(C_5H_7O_2)_3$ produced at least 10 different compounds (see Table 1). The Al_2O_3 films produced under direct decomposition conditions were black. The black color is consistent with previous observations that films produced from direct pyrolysis contained carbon.[6−10]

The formation of Al_2O_3 films from the pyrolysis of $Al(C_5H_7O_2)_3$ followed at least two pathways and had steps in the reaction mechanism that follow the Langmuir mechanism. However, the rate limiting step could occur in the gas phase since the activation energy is fairly large. The induction period observed by Minkina[12] and the nonlinear initial Langmuir region observed here could also indicate that a gas-phase product forms first. This product could then react on the surface. Bykov et al.[14] proposed that $Al(C_5H_7O_2)_2OH$ could be one of the initial products formed via

$$Al(C_5H_7O_2)_3 \leftrightarrow Al(C_5H_7O_2)_2OH + C_5H_6O \quad (14)$$

This intermediate could also be produced from the reaction with water

$$Al(C_5H_7O_2)_3 + H_2O \leftrightarrow Al(C_5H_7O_2)_2OH + C_5H_8O_2 \quad (15)$$

The $Al(C_5H_7O_2)_2OH$ could then react on the surface via pathways such as

$$2Al(C_5H_7O_2)_2OH \rightarrow Al_2O_3 + 2C_5H_8O_2 + 2C_5H_6O + H_2O \quad (16)$$

or

$$2Al(C_5H_7O_2)_2OH + H_2O \rightarrow Al_2O_3 + 4C_5H_8O_2 \quad (17)$$

All of the proposed organic products were observed and can form through the stepwise transfer of protons. Support for this mechanism include steps 15 and 17 being first order in the H_2O pressure and permitting varying concentrations of $C_5H_8O_2$ and C_5H_6O to form as the amount of H_2O in the system changes.

The other products observed could be produced from the $Al(C_5H_7O_2)_2OH$. The thermal decomposition of the bis 2,4-pentanedionato complexes of the group II metals proceeds exclusively through loss of 2-propanone to form the 2,4,6-heptanetrionate as an intermediate:[18]

$$M(C_5H_7O_2)_2 \rightarrow C_3H_6O + M(C_7H_8O_3) \qquad (18)$$

The 2,4,6-heptanetrionate reacted with bis 2,4-pentanedionato complex to form 3,5-dimethylphenol through the loss of 2-propanone via a reaction something like

$$M(C_5H_7O_2)_2 + 2M(C_7H_8O_3) + H_2O \rightarrow 2C_8H_{10}O + 2C_3H_6O + 2MCO_3 + MO \qquad (19)$$

Decomposition of the 3,5-dimethyl phenol generated methane and carbon.

$$C_8H_{10}O \rightarrow 2CH_4 + H_2O + 6C \qquad (20)$$

It is likely that a similar pathway also produced these compounds during the decomposition of the $Al(C_5H_7O_2)_2$-OH. The remaining compounds observed in the mass spectrum of the products could form from dimerization of the C_5H_6O or as intermediates in the cyclicization reaction suggested by reaction 19. The ketene could form from the decomposition of these cyclicization intermediates or from the decomposition of a gaseous product.

The kinetic investigations indicate that reactions 14 and 16 have lower activation energies than reaction 14 and 16 and dominate the mechanism at low temperatures if an excess of water vapor is present.

Previous research[14] has established that equilibrium (or near equilibrium) conditions can be established for water reactions by using restricted flow conditions. If the $Al(C_5H_7O_2)_3$ is adsorbed on the surface during the reaction, the overall reaction would be

$$2Al(C_5H_7O_2)_3(sur) + 3H_2O(g) \rightarrow Al_2O_3(s) + 6C_5H_8O_2(g) \qquad (21)$$

Assuming that all solids have unit activity and that the gases behave ideally, the equilibrium constant for this reaction is

$$K = P^6(C_5H_8O_2)/P^3(H_2O) \qquad (22)$$

Since the partial pressure is proportional to the sample absorbance, the equilibrium constant becomes[11,14,17]

$$K = BA^6(C_5H_8O_2)/A^3(H_2O) \qquad (23)$$

where B is a collection of proportionality constants and A is the absorbance of the indicated compound. Plotting $\ln(A^6(C_5H_8O_2)/A^3(H_2O))$ verses the reciprocal of the temperature is expected to give a straight line with slope equal to $\Delta_{RXN}H/R$ if equilibrium has been established.

(18) Kippeny, T. A.; Shickel, J. A.; Parrett, Jr., J. W.; Arthur, J. A.; DeVore, T. C. *Chem. Mater.*, to be submitted.

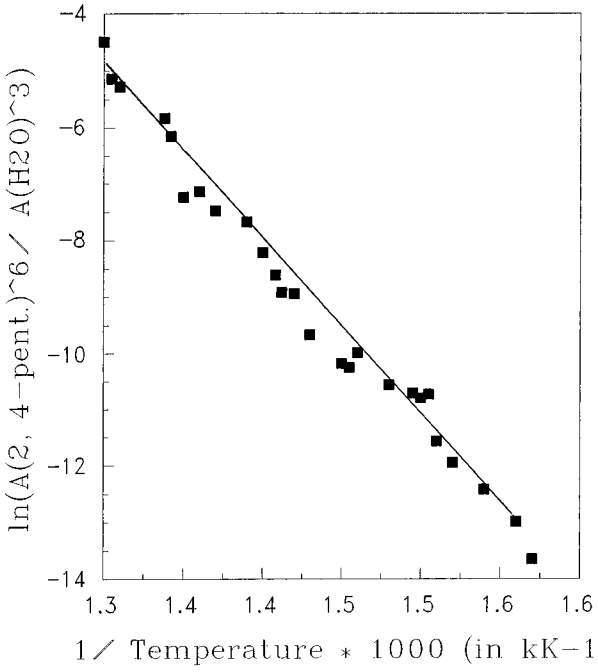

Figure 11. van't Hoff plot for the reaction between tris(2,4-pentanedionato)aluminum and a water vapor using restricted flow conditions.

As shown in Figure 11, a good straight line was obtained under restricted flow conditions with a large water flow with $\Delta_{RXN}H = +245 \pm 5$ kJ/mol. On the basis of the literature values for Δ_fH of $C_5H_8O_2(g)$ (−386.6 kJ/mol),[19] $H_2O(g)$ (−241.9 kJ/mol),[20] and $Al_2O_3(s)$ (−1675.7 kJ/mol),[20] the calculated value for $\Delta_fH(Al(C_5H_7O_2)_3(sur))$ was -1757 ± 5 kJ/mol. This value is in good agreement with the value of −1749 kJ/mol reported for $\Delta_fH(Al(C_5H_7O_2)_3(s)$ by Kawasaki.[21] $\Delta_{ADS}H$ for $Al(C_5H_7O_2)_3$ is calculated to be approximately -8 ± 5 kJ/mol, indicating that the $Al(C_5H_7O_2)_3$ was weakly bound (physiadsorbed) on the surface (probably of $Al_2O_3(s)$).

Conclusions

The production of Al_2O_3 from $Al(C_5H_7O_2)_3$ during CVD processes followed at least two different reaction pathways. The lowest energy pathway involved the reaction between $Al(C_5H_7O_2)_3$ and water. This reaction occurred at relatively low temperatures, had an apparent activation energy of 28 kJ/mol, and produced carbon-free Al_2O_3 films and 2,4-pentanedione as the main products. The second pathway involved the thermal decomposition of the $Al(C_5H_7O_2)_3$, had a higher apparent activation energy (~100 kJ/mol for the initial product and more for other products), produced an Al_2O_3 film contaminated with carbon, and formed several organic byproducts. Adding water to the reaction mixture favored the first process but did not prevent the decomposition pathway from occurring over the temperature ranges used during typical CVD processes.

Acknowledgment. The authors wish to thank ACS PRF for their support of this project.

CM960504P

(19) Melia, T.; Merrifield, R. *J. Appl. Chem.* **1969**, *19*, 79−82.

(20) Chase, Jr., M. W.; Davies, C. A.; Downey, Jr., J. R.; Frurip, D. J.; McDonald, R. A.; Syverud, A. N. *J. Phys. Chem. Ref. Data* **1985**, 14.

(21) Kawasaki, Y.; Tanaka, T.; Okawara, R. *Technol. Rept. Osaka University* **1963**, *13*, 217−22.